ORIGINAL ARTICLE

Glass transition at the polystyrene/polyethylene glycol interface observed via contact angle measurements

Takashi Sasaki[1] · Kazuaki Hiraki[1] · Aizzahtul Athirah[1] · Kodai Matsuta[1] · Natsuki Takeuchi[1]

Abstract

We investigated the possibility of detecting the interfacial glass transition of a polymer with static contact angle measurements of a liquid polyethylene glycol on the polymer surface. The observed contact angle θ reflects the deviation from an equilibrium state at low temperatures, and the temperature dependence of $\cos \theta$ changes discontinuously at the interfacial glass transition temperature T_g, manifesting a change in the interfacial entropy. This outcome was demonstrated experimentally for a liquid of polyethylene glycol (PEG) on an atactic polystyrene (PS) surface. The evaluated T_g was ca. 362 K. This value is lower than a calorimetric T_g for a bulk PS. This difference reflects molecular interactions at the interface, indicating that the T_g obtained from the contact angle measurement is sensitive to the dynamics near the polymer/liquid interface.

Introduction

Since the first discovery of anomalous glass transition behaviors in ultrathin polymer films, much attention has been focused on the dynamics of nanosized polymeric materials [1–5]. The anomaly concerns the fundamental issue of the glass transition mechanism, which concerns prominent viscous slowdown during cooling in supercooled liquids [6, 7]. Despite the intense effort exerted to date to understand the nature of the dynamics in nanosized polymers, the nature of these dynamics is still an open question because of the wide variety of experimental observations [5]. Nevertheless, there is considerable evidence for the existence of a characteristic layer near the surface and the interface [5, 8–10] that is responsible for the size-dependent glass transition temperature (T_g) in polymer thin films. Thus there has been a growing interest on surface and interfacial glass transition.

Contact angle measurements can detect the properties of the interfacial region of materials [11], and in this sense, they may be suitable for detecting the interfacial glass transition. Since the glass transition is related to the dynamical properties of a material, T_g can be determined by dynamical measurements that are associated with a certain time constant. To evaluate the differences between the dynamics at the surface (or interface) of the polymer and that of its bulk (interior part of the material), dynamical measurements at the interface are needed. To date, direct observation of the wetting process of liquids on the polymer surface has been carried out [12–15]. Dupas et al. found that the wetting velocity of a solvent decreases when the polymer substrate is transformed from a glassy state to the liquid state [15]. Zuo et al. evaluated the glass transitions of polymer thin films by detecting a stick-slip behavior of a liquid wetting the film surface [16]. Furthermore, the rheological properties in the surface region of polymer thin films were investigated through the growth of the so-called wetting ridge phenomenon [17, 18]. These are purely dynamical observations at the polymer/liquid interface. On the other hand, static measurement of interfacial tension such as contact angle measurements, might be insensitive to the interfacial glass transition, because they do not detect any dynamics. In addition, the observed quantity (interfacial tension) is a thermodynamic parameter that is in principle meaningful only at equilibrium (glassy state is nonequilibrium). Nevertheless, actual observed values of the contact angle may be susceptible to the interfacial glass transition to some extent: the observed

value can reflect the deviation from a quasi-equilibrium (supercooled) value at temperatures lower than T_g so that the onset of this deviation gives the interfacial T_g. One example is the heat capacity of a supercooled liquid, which undergoes a discontinuous reduction on cooling at T_g (calorimetric T_g). In this case, the cooling rate determines the time constant of the measurement. Similarly, the temperature dependence of a polymer/liquid interfacial tension possibly provides some indication of vitrification. Thus it is possible to detect the interfacial glass transition via contact angle measurements.

The time constant of the glass transition observation through the contact angle measurement may be related to the initial wetting (equilibration) process following the placement of the droplet on the polymer substrate. The time required for the contact angle to reach a constant value depends on the temperature. The contact angle values at a fixed time may exhibit a change in their temperature dependence at a certain temperature that corresponds to a T_g with a time constant of the above fixed time. The time-evolution of the initial wetting process may provide information regarding the relaxation processes at the polymer/liquid interface. If the wetting process is affected by the segmental dynamics of the polymer substrate, it will change discontinuously at T_g. At temperatures above T_g, the viscoelasticity that concerns segmental dynamics at the polymer interface may affect the wetting process to some extent. We should also note that the interfacial tension reflects the structure and molecular processes at the interface such as penetration and swelling on the nanoscale [12, 14, 19]. Structural studies of the polymer interface have revealed characteristic conformational states induced by nonsolvents [20–23] that alter the polymer dynamics at the interface [14, 24]. The interfacial tension observed through the contact angle measurement is expected to reflect the specific properties at the polymer/liquid interface.

In this study, we investigate the possibility of observing the interfacial glass transition through static contact angle measurements of a nonsolvent droplet on a polymer surface at a fixed elapsed time. The temperature dependence of the contact angle on an atactic polystyrene (PS) surface was evaluated. Furthermore, time-evolution of the contact angle was examined to evaluate the relaxation time during the equilibration (wetting) of the liquid droplet to check if the observed wetting reflects the interfacial glass transition. In the next section, we discuss the possible detection of T_g based on thermodynamics.

Thermodynamic principles

We first consider the temperature dependence of interfacial tension (interfacial free energy) based on thermodynamics. The interfacial tension at a polymer/liquid interface can be evaluated from the contact angle of a liquid droplet (nonsolvent). In this case, the polymer/liquid interfacial tension γ_{pl} obeys the well-known Young equation

$$\gamma_{ap} = \gamma_{pl} + \gamma_{al} \cos \theta \tag{1}$$

where θ is the contact angle, and γ_{ap} and γ_{al} are the interfacial tensions of the air/polymer and air/liquid interfaces, respectively. The temperature dependence of interfacial tension is related to interfacial entropy S_σ (per unit area) for a homogeneous interface according to

$$\left(\frac{\partial \gamma}{\partial T}\right)_A = -S_\sigma \tag{2}$$

where A is the interfacial area. Based on the Gibbs ideal interface assumption (zero volume interfacial phase), Eq 2 is derived when the dividing plane is located such that the interfacial excess becomes zero [25]. Equation 2 is generally valid for a binary system (such as the present polymer/liquid interface), in which the interfacial excess for both components becomes zero at a common dividing plane. We note here that S_σ is the contribution from the interface to the total entropy of the binary phase system, and thus its value can be either positive or negative.

It is known that the surface tension of regular liquids decreases almost linearly with increasing temperature over a temperature range of at least several tens of K [26]. This behavior is also the case for polymeric liquids [27, 28]. This outcome indicates that generally, the surface entropy is positive and its temperature dependence is very weak (almost constant). This tendency is probably characteristic of the liquid/gas interface, where the entropy difference between the two contacting phases is very large, and the molecular interactions between the liquid and gas molecules do not play an important role in determining the temperature dependence of γ. By contrast, at a polymer/liquid interface, the molecular interactions between the two species may significantly contribute to the entropy of the system. When the polymer is in a supercooled liquid phase (above T_g), the interactions at the interface can in some cases be so strong that the interfacial entropy becomes negative. On the other hand, below T_g, the configuration of the polymer phase is kinetically frozen, preventing molecular rearrangements that would make the interactions become effective with favorable molecular packing structures. This outcome leads to an apparently weaker polymer/liquid interactions, and the interfacial contribution to the total entropy becomes very small for $T < T_g$ ($S_\sigma \sim 0$). When the polymer/liquid interaction is so strong for $T > T_g$ that it forces some specific configurations to occur at the interface, S_σ may be negative. As a result, a discontinuous change in S_σ is expected at T_g.

Based on the above consideration, the general trends for the temperature dependence of the interfacial tensions are
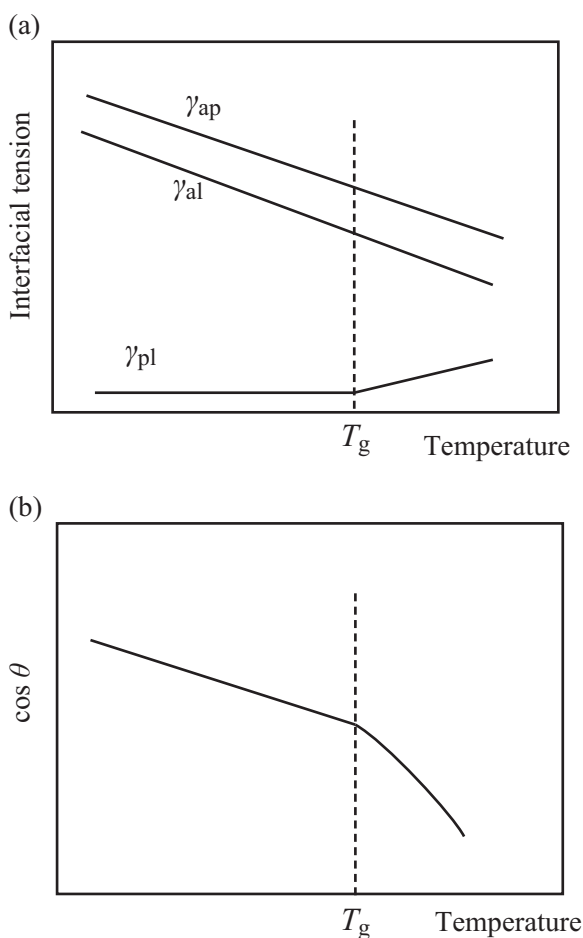
(a)

(b)

Fig. 1 Predicted temperature profiles of the interfacial tensions and contact angle (cos θ)

expected to be as shown in Fig. 1. It is assumed that the surface tension of the polymer γ_{ap} is not influenced by its glass transition because of the weak molecular interaction at the surface. For Fig. 1a, it is also assumed that S_σ at the polymer/liquid interface is negative as may be expected when strong molecular interactions between the polymer and liquid are present. The interfacial tension at the polymer/liquid interface γ_{pl} exhibits an upward kink (break point) at T_g where a discontinuous change of S_σ occurs. Accordingly, the temperature dependence of cos $\theta = (\gamma_{ap} - \gamma_{pl}) / \gamma_{al}$ changes at T_g as shown in Fig. 1b. From this change in the temperature dependence of cos θ, one can evaluate the interfacial T_g. The jump of S_σ at T_g is analogous to that of the isobaric heat capacity C_p typically observed by differential scanning calorimetry (DSC). Indeed, S_σ is a temperature derivative of the interfacial free energy (interfacial tension), while C_p is a temperature derivative of the enthalpy. The temperature derivative of energy generally undergoes discontinuous change at T_g, while energy parameters such as interfacial tension and enthalpy are continuous at T_g. The discontinuous change of the temperature

dependence reflects the deviation from a quasi-equilibrium state below T_g for the experimentally observed values with a certain time constant.

Experimental

Atactic PS ($M_n = 1530$ kDa, $M_w = 1571$ kDa) was purchased from Scientific Polymer Products (Ontario, NY, USA) and was used without further purification. The glass transition temperature (bulk T_g) of this polymer was obtained as 378.5 K via DSC at a heating rate of 20 K min^{-1}. Cast PS films were prepared on glass substrates from a 1.0 wt% solution of PS in tetrahydrofuran or toluene. Prior to use, the glass substrates were cleaned as follows: the substrates were sonicated in a 0.2% aqueous solution of an alkaline detergent for 30 min, rinsed with pure water, sonicated in methanol for 20 min, rinsed again with methanol, and then dried at 50 °C for 1 h under atmospheric pressure. The cast PS films were dried under vacuum for 24 h. Some of the films were further annealed at 413 K for 4 h under vacuum to examine the nonequilibrium effects of the cast film. The surface roughness of the films was evaluated with an atomic force microscope (AFM) Seiko Instruments (Chiba, Japan) Nano Navi. Topography images were obtained in the tapping mode with the scan dimensions of 1 μm × 1 μm and a scan rate of 1 Hz.

The thickness of the obtained films ranged from 1 to 3 μm. For the contact angle measurements, a low molecular weight polyethylene glycol (PEG) ($M_w = 570$–630 Da) purchased from Nacalai Tesque (Kyoto, Japan) was used without further purification. This polymeric liquid is non-volatile and has an appropriate surface tension value that is suitable for our contact angle measurements. In the analysis, we used literature data for the surface tension of atactic PS [29]. For the low molecular weight PEG, we used 43.5 mN m^{-1} at 20 °C and –0.1170 mN m^{-1} K^{-1} for the temperature coefficient [30]. The temperature dependence of the PEG was measured using an Ostwald's viscometer.

Contact angle measurements were performed by using a homemade apparatus that consists of a temperature-controlled stage and a CCD camera equipped with a zoom lens (Edmund Scientific). The axis of the camera was slightly inclined upward from the horizontal axis to observe a reflection image on the substrate surface that allowed the precise determination of the contact point of the droplet. Fig. 2 shows typical droplet images. The observed shapes of the droplets were revealed to be nearly spherical as shown by the dotted lines in Fig. 2, and the contact angle was evaluated from the shape based on a geometrical relation [12]. The calibration for the temperature at the interface with respect to the preset temperature was carefully carried out by directly measuring the temperature of the droplet
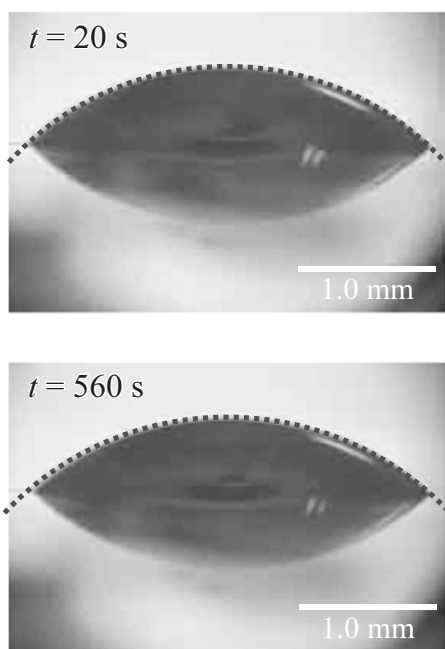
Fig. 2 Typical images of a PEG droplet on a PS film at 393 K at $t = 20$ and 560 s. The dotted curves indicate fitted circles, suggesting that the shape of the droplet is close to a spherical cap

with an ultrathin needle thermocouple. PEG (2.0 µL) was placed on a PS film of which the temperature had been settled, and the image of the formed droplet was taken every 10 s to obtain the contact angle time-evolution data. The elapsed time was recorded after the droplet was initially placed on the polymer surface. To check the reproducibility of the data, the measurements were repeated 3–8 times at each temperature (40–152 °C), and standard deviation for $\cos \theta$ was evaluated from the multiple measurements.

It should be noted that generally, the experimentally observed contact angle is not for an equilibrium (quasi-equilibrium) state: the contact angle exhibits hysteresis, e.g., the difference between the advancing and receding angles. It is difficult to achieve the equilibrium state for the polymer/liquid/air ternary system even above T_g. Accordingly, we should consider that the observed contact angle is obtained under certain specific conditions with the system found in one of the possible metastable states even after the wetting process is completed. Therefore, we had to be careful to realize identical experimental conditions, in particular, for the manner of placing the droplet on the surface by controlling the injection rate of the liquid from a syringe and the timing of the removal of the syringe-needle from the droplet in order to obtain reproducible results.

It was preferable to use the high molecular weight PS (1,530 kDa) for the contact angle measurement that in principle requires a rigid substrate. The film of the present PS was sufficiently stable to be regarded as a solid-like substrate in the present temperature range (above T_g), allowing contact

angle measurement. We also confirmed via optical microscopy that no apparent deformation of the contact line occurs during wetting within 10 min even at 413 K.

Results and Discussion

Figure 3 shows the typical time variation profiles of $\cos \theta(t)$ for a non-annealed PS substrate. The profiles of $\cos \theta(t)$ at lower temperatures are shown in Figs. S2–S6, where the time evolution occurs too slow to explicitly evaluate θ_∞ [see Supplementary Material]. The contact angle generally decreases ($\cos \theta$ increases) with time, and at lower temperatures (<390 K) it appears to approaches an asymptotic value θ_∞. The decreasing θ indicates surface wetting process of the liquid. Based on the analysis of the observed images, we confirmed that within the experimental error, the volume of the droplet does not change significantly with time up to 600 s. This indicates that no significant absorption of the liquids into the PS phase occurs. Additionally, it is likely that neither the evaporation of the liquid nor the absorption of atmospheric water into the liquid occurs. However, some microscopic swelling may occur at high temperatures above T_g, as described below. On the other hand, molecular rearrangements on a microscopic scale at the interface that contribute to the reduction of the observed contact angle may occur. The curve of $\cos \theta(t)$ for PS/PEG at a high temperature (400 K) shows an exceptionally slow increase, which may be due to thermal degradation of PEG [31].

Figure 4 shows $\cos \theta$ observed at 600 s with respect to temperature. A turnoff point (kink) that may be a manifestation of the glass transition at the interface is seen for both liquids, as predicted in Fig. 1.

Nonequilibrium features of polymer thin films such as residual stresses have been reported to affect their various dynamical behaviors, in particular for spin-cast films [32, 33]. To assess such nonequilibrium effects for the present solvent-cast films, we compared the results for the films annealed at 413 K for 4 h and the non-annealed films., The data for both the annealed and non-annealed PS are plotted in Fig. 4. Perhaps unexpectedly, we found no significant difference between the annealed and non-annealed films within the experimental error. Furthermore, we investigated the surface topology that is a crucial factor in the contact angle measurement of these PS films. Table 1 shows the surface roughness R evaluated from AFM measurements. Here R is the root mean square height defined as

$$R = \sqrt{\frac{1}{n}\sum_{i}^{n} h_i^2} \tag{3}$$

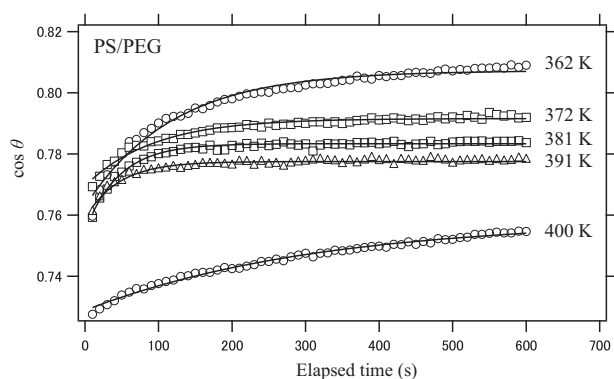where h_i is the height deviation at position i. The AFM images are shown in Fig. S1 [see Supplementary Material].

Fig. 3 Typical time-evolution profiles of the contact angle (cos θ) of the PEG droplet on the PS surface (without annealing) at different temperatures. The solid curves indicate the results of the fitting with Eq. 4

We found that the surface of the present solvent-cast films is very smooth compared with spin-cast films: for the latter, R ranges from 1.0 to 4.7 nm depending on the preparation condition. The surface roughness data in Table 1 support the fact that the annealing induces no significant change in the contact angle measurements. We found that the pre-annealing does not alter the transition temperature within the present experimental error.

The kink temperature observed in Fig. 4 was evaluated to be approximately 362 K by linear regression analysis, with two regression lines determined for $T < 360$ K and $T > 378$ K. The observed kink is considered to be the corresponding interfacial glass transition temperature. We found that a kink in the cos θ vs. temperature profile also occurs for other polymers. For example, low molecular weight poly(α-methylstyrene) and poly(4-*tert*-butylstyrene) exhibit kinks at approximately 320 K and 355 K, respectively, both of which are lower than their bulk calorimetric T_g (369 K and 413 K, respectively). The results are shown in Figs. S7 and S8 [see Supplementary Material]. Incidentally, poly(α-methylstyrene) is known to exhibit no mobile surface layer [34, 35]; this still appears to be a mystery.

Since T_g is a kinetic parameter, the observed values depend on the time scale of the measurements. The time constant for the present contact angle measurement is determined by the elapsed time, i.e., 600 s for the data in Fig. 4. This time is longer than that for a typical DSC scan: the time constant for a temperature scanning rate of 20 K min^{-1} is estimated to be ca. 30 s based on the Frenkel–Kobeko–Reiner relation [36, 37]. Even considering the above difference in the time constant, the T_g values obtained from Fig. 4 are still lower than the calorimetric T_g of the bulk PS (378.5 K): a variation of the time constant of one decade leads to a T_g shift of just several K for PS. Therefore, it is likely that the lower T_gs obtained here may reflect the interfacial segmental dynamics of PS with higher
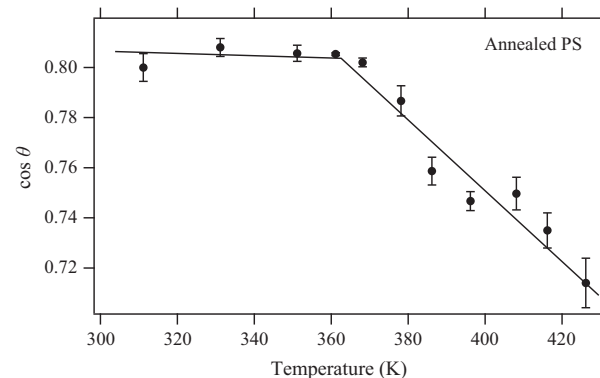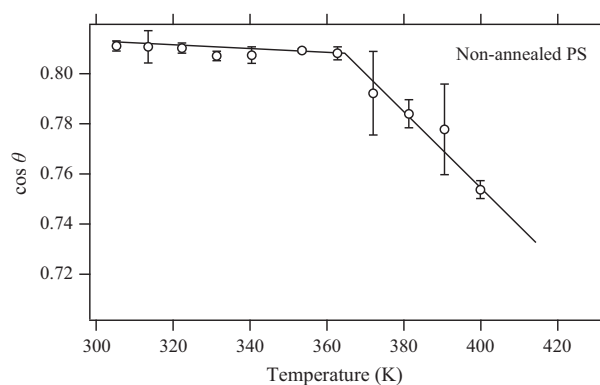

Fig. 4 Contact angle (cos θ) at an elapsed time of 600 s for the PEG droplet on the PS substrates that were annealed at 413 K for 4 h (annealed PS), and on the PS substrates without annealing (non-annealed PS)

Table 1 Surface roughness of the solvent-cast polystyrene films

annealing	R / nm
Not annealed	0.30
413 K, 4 h	0.30
413 K, 4 h with PEG	1.1–1.5

mobility, and the present contact angle measurement detects the interfacial glass transition. It is expected that the kink temperature will be higher at shorter elapsed times. We found that this dependence is actually rather weak within the present time window (600 s): for example, at 50 s the kink was evaluated to be 365 K, which is only slightly higher than that at 600 s (362 K). This weak tendency may be consistent with the relatively high fragility of polystyrene.

We should also note that the interfacial T_g depends on the identity of the liquids. There is considerable evidence that the molecular interactions at polymer/nonsolvent interface give rise to specific structures and dynamics near the interface [14, 20–24]. Each interaction may have different strengths, which may lead to different time constants of intermolecular rearrangement near the interface.
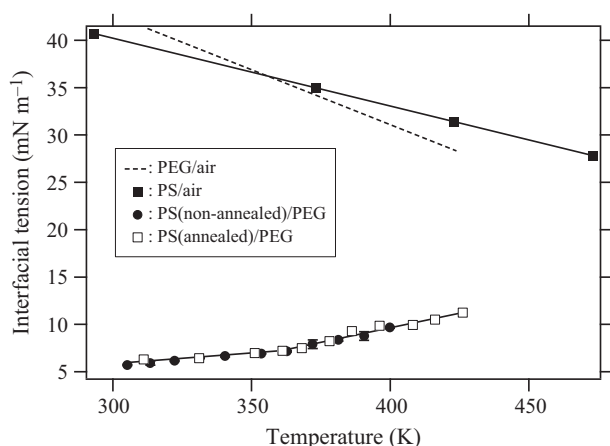
Fig. 5 Interfacial tensions vs. the temperature. The values for γ(PS/PEG) were evaluated from $\cos\theta$, γ(PEG/air), and γ(PS/air). The values for γ(PEG/air) and γ(PS/air) are based on the literature data. The solid lines were obtained via linear regression analysis

The probe liquid PEG is a nonsolvent for PS at least at room temperature (no macroscopic swelling was observed). However, some microscopic swelling at the interface was suggested to occur at a temperature above the bulk T_g. The PS surface that had contacted with PEG at 413 K for 4 h exhibited higher surface roughness as shown in Table 1: its R-value is greater than that for the non-annealed surface or that for the surface annealed without contacting the probe liquid. For the above-annealed sample with PEG, AFM measurements were made after the removal of the PEG by rinsing with methanol, followed by drying under vacuum at room temperature for 24 h. The kink observed in Fig. 4 may be affected by the above microscopic swelling, which requires segmental rearrangements of PS at the interface. It is strongly suggested that the interactions between PS and PEG affect the observed glass transition that is specific to the interface.

Figure 5 shows the interfacial tensions for the air/PEG, air/PS, and PS/PEG interfaces plotted against the temperature. The interfacial tension γ of PS/PEG was obtained from $\cos\theta$, γ(PEG/air), and γ(PS/air), with the latter two variables evaluated based on the literature data as mentioned in the experimental section. The profiles of γ(PS/PEG) exhibit an upward turnoff at T_g. The lower γ for PS/PEG may originate from the relatively strong interactions at the interface discussed above, due to which the molecules near the interface assume configurations (molecular packings) with lower potential energies. The interfacial entropy S_σ was evaluated from the slope of γ(PS/PEG) against temperature and was found to be -0.019 (below T_g) and -0.061 mJ m^{-2} K^{-1} (above T_g). The negative values imply that the interface contributes to decreasing the total entropy of the polymer/PEG system. The obtained value of S_σ is larger for $T < T_g$ than for $T > T_g$. Below T_g, the configuration of PS at the interface is in a nonequilibrium state, which is less influenced by the contacting liquid phase. By contrast, at temperatures above T_g, the PS configurations are easily optimized to achieve a stable interfacial state (quasi-equilibrium state), resulting in a lower interfacial entropy than that for $T < T_g$.

The change of the interfacial entropy at T_g may be interpreted based on the molecular interactions. Surface tension is generally governed by the cohesive energies consisting of the contributions of various molecular interactions such as dispersion, polar, induction, hydrogen bonding, and acid–base interactions [19, 38]. Similarly, the contributions of these interactions across the interface are considered to determine the interfacial tension (free energy) for a polymer/liquid system. The interfacial tension may be represented by an adhesion energy E_{pl}, i.e., $\gamma_{pl} = \gamma_{ap} + \gamma_{al} - E_{pl}$ [19]. E_{pl} can be expressed as $E_{pl} = \Phi(\gamma_{ap}\,\gamma_{al})^{1/2}$, where Φ is a factor related to the interaction between the two species [39]. Here, Φ is sensitive to the polymer/liquid interactions, and this factor is considered to undergo a discontinuous change at T_g.

Zuo et al. found that stick-slip behaviors during wetting occurs in the temperature range of the glass transition and revealed that the T_g obtained by this method depends on the thickness of the substrate PS films below ca. 100 nm and depends on the chemistry of the substrate supporting the film [16]. This result suggests that such dynamic wetting measurements detect the viscoelastic behaviors of the entire polymer film, i.e., the observed stick-slip behavior is sensitive to the thickness of the film and is even sensitive to the other side of the film interface (polymer/substrate). Additionally, the wetting ridge phenomenon reflects the dynamics of the deformation near the polymer surface that involves a surface region with a depth of at least a few tens of nm [17, 18]. On the other hand, the static contact angle is essentially a parameter that is related exclusively to the polymer/liquid interface and it might not be very sensitive to the thickness. However, it was reported that the surface tension of spin-cast PS thin films depends on their thickness in the range of 86–359 nm [40]. To evaluate the thickness of the interfacial region that is detected by the contact angle measurements, investigations with thinner polymer films should be performed.

The time-evolution of $\cos\theta(t)$ represents the wetting dynamics of the liquids on PS surface. To evaluate the time constant of the wetting τ, the $\cos\theta(t)$ profiles in Fig. 3 were fitted with an empirical equation

$$\cos\theta(t) = \cos\theta_\infty[1 - b\,exp(-t/\tau)] \qquad (4)$$

where θ_∞ is the asymptotic value of the contact angle, and b is a nondimensional parameter. When plotted against the temperature, the values of $\cos\theta_\infty$ obtained from the analysis exhibited a similar profile to that in Fig. 4: there was still a break point near T_g. This result suggests that the observed θ_∞ is still an apparent value that reflects the present specific

experimental conditions rather than the ultimate value that corresponds to a quasi-equilibrium state.

Figure 6 shows Arrhenius plots for τ. At temperatures higher than T_g, a nearly Arrhenius behavior is observed. We should note here that the plot in Fig. 6 does not exhibit a kink at T_g in contrast to Fig. 4, because τ is the relaxation time for reaching the asymptotic contact angle, and therefore in principle, τ should not depend on any time constants of measurement. The apparent activation energy E_a for the wetting dynamics was evaluated via linear regression analysis to be 32.8 kJ mol^{-1}, while the activation energy of viscosity E_η for PEG was evaluated as 30.8 kJ mol^{-1}. The obtained E_a is similar to (or slightly greater than) the E_η value. This result suggests that the wetting dynamics is largely governed by the molecular process of the liquid droplet as has been discussed analytically in ref. [41].

In an extreme case, if the PS chain dynamics at the interface were completely incorporated in the wetting process, the apparent activation energy would be nearly $E_{PS} + E_\eta$, where E_{PS} is the activation energy of the PS segmental dynamics. E_{PS} for bulk PS is generally much higher than the obtained E_a: from a typical value of fragility parameter for atactic bulk PS [42–44], E_{PS} at T_g is estimated to be 1.0×10^3 kJ mol^{-1}. This estimation suggests that the wetting dynamics is not strongly linked to the segmental dynamics of the PS phase. Nevertheless, there may be some interfacial interactions that at least weakly affect the wetting behavior. This may be supported by the enhanced surface roughness shown in Table 1. The slightly enhanced activation energy of E_a from E_η might indicate that the PS/PEG interactions belong to an intermediate region between the two limits of diffusion and low-friction of Kramers [45, 46]. The present contact angle measurements can provide a signature of the glass transition at the interface, and this does not contradict the considerations based on thermodynamics as discussed previously. The detection of glass transition appears to be possible only when the polymer/liquid interactions affect the wetting process to some extent.

Conclusions

In this study, we observed a discontinuous change in the temperature dependence of the contact angle for PS/PEG/air ternary systems that was attributed to the signature for the glass transition at the interface of PS/PEG. It should be noted that the contact angle values obtained by static measurements are not the ultimate values at equilibrium. In addition, even if such ultimate values were obtained, they would not exhibit any signals for T_g because the contact angle is not a dynamical parameter in principle. In contrast, the actually observed values of the contact angle are not the
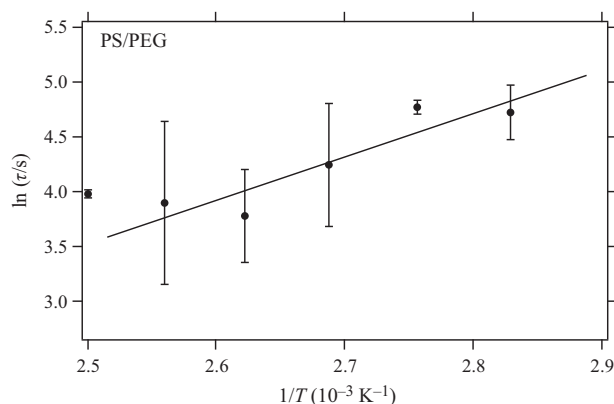

Fig. 6 Arrhenius plot of the time constant τ for wetting obtained from the cos θ vs. time profiles. The solid line was obtained from the linear regression analysis

equilibrium values for $T < T_g$, and are associated with a certain time constant of the measurement (e.g., 600 s for the data in Fig. 4). The deviation from the ultimate value becomes significant below T_g, reflecting the frozen segmental dynamics of the PS phase. The observed temperature profiles for the contact angle in Fig. 4 imply that the apparent interfacial entropy changes discontinuously at T_g. We found that the interfacial T_g at PS/PEG is lower than the calorimetric T_g. This finding strongly suggests that the evaluated T_g reflects the molecular interaction at the interface. The thickness of the interfacial region that is reflected in the present T_g values is currently unknown. To elucidate this characteristic thickness, further investigations of polymer thin films with different thicknesses below 100 nm should be performed.

Author contributions TS designed and supervised the research. KH, AA, and KM carried out the contact angle measurements and data analysis. NT carried out the AFM measurements. TS wrote the paper.

Compliance with ethical standards

References

1. Keddie JL, Jones RAL, Cory RA. Size-dependent depression of the glass transition temperature in polymer films. Europhys Lett. 1994;27:59–64.
2. Forrest JA, Dalnoki-Veress K. The glass transition in thin polymer films. Adv Colloid Interface Sci. 2001;94:167–96.

3. Alcoutlabi M, McKenna GB. Effects of confinement on material behaviour at the nanometre size scale. J Phys, Cond Matter. 2005;17:R461–524.

4. McKenna GB. Ten (or more) years of dynamics in confinement: Perspectives for 2010. Eur Phys J Spec Top. 2010;189:285–302.

5. Napolitano S, Glynos E, Tito NB. Glass transition of polymers in bulk, confined geometries, and near interfaces. Repts Progr Phys. 2017;80:036602.

6. Debenedetti PG, Stillinger FH. Supercooled liquids and the glass transition. Nature. 2001;410:259–67.

7. McKenna GB, Simon SL. Challenges in the dynamics and kinetics of glass-forming polymers. Macromolecules. 2017;50:6333–61.

8. Tanaka K, Takahara A, Kajiyama T. Rheological analysis of surface relaxation process of monodisperse polystyrene films. Macromolecules. 2000;33:7588–93.

9. Akabori K, Tanaka K, Nagamura T, Takahara A, Kajiyama T. Molecular motion in ultrathin polystyrene films: dynamic mechanical analysis of surface and interfacial effects. Macromolecules. 2005;38:9735–41.

10. Ediger MD, Forrest JA. Dynamics near free surfaces and the glass transition in thin polymer films: a view to the future. Macromolecules. 2014;47:471–8.

11. Zisman WA. Relation of the equilibrium contact angle to liquid and solid constitution. Adv Chem. 1964;43:1–51.

12. Farris S, Introzzi L, Biagioni P, Holz T, Schiraldi A, Piergiovanni L. Wetting of biopolymer coatings: Contact angle kinetics and image analysis investigation. Langmuir. 2011;27:7563–74.

13. Muralidhar P, Bonaccurso E, Auernhammer GK, Butt H-J. Fast dynamic wetting of polymer surfaces by miscible and immiscible liquids. Colloid Polym Sci. 2011;289:1609–15.

14. Horinouchi A, Atarashi H, Fujii Y, Tanaka K. Dynamics of water-induced surface reorganization in poly(methyl methacrylate) films. Macromolecules. 2012;45:4638–42.

15. Dupas J, Verneuil E, Van Landeghem M, Bresson B, Forny L, Ramaioli M, et al. Glass transition accelerates the spreading of polar solvents on a soluble polymer. Phys Rev Lett. 2014;112:188302.

16. Zuo B, Qian C, Yan D, Liu Y, Liu W, Fan H, et al. Probing glass transitions in thin and ultrathin polystyrene films by stick-slip behavior during dynamic wetting of liquid droplets on their surfaces. Macromolecules. 2013;46:1875–82.

17. Zuo B, Tian H, Liang Y, Xu H, Zhang W, Zhang L, et al. Probing the rheological properties of supported thin polystyrene films by investigating the growth dynamics of wetting ridges. Soft Matter. 2016;12:6120–31.

18. Sun S, Xu H, Han J, Zhu Y, Zuo B, Wang X, et al. The architecture of the adsorbed layer at the substrate interface determines the glass transition of supported ultrathin polystyrene films. Soft Matter. 2016;12:8348–58.

19. Chaudhury MK. Interfacial interaction between low-energy surfaces. Mater Sci Eng. 1996;R16:97–159.

20. Yang CSC, Wilson PT, Richter LJ. Structure of polystyrene at the interface with various liquids. Macromolecules. 2004;37:7742–6.

21. Tanaka K, Fujii Y, Atarashi H, Akabori K, Hino M, Nagamura T. Nonsolvents cause swelling at the interface with poly(methyl methacrylate) films. Langmuir. 2008;24:296–301.

22. Tateishi Y, Kai N, Noguchi H, Uosaki K, Nagamura T, Tanaka K. Local conformation of poly(methyl methacrylate) at nitrogen and water interfaces. Polym Chem. 2010;1:303–11.

23. Horinouchi A, Yamada NL, Tanaka K. Aggregation states of polystyrene at nonsolvent interfaces. Langmuir. 2014; 30:6565–70.

24. Fujii Y, Nagamura T, Tanaka K. Relaxation behavior of poly (methyl methacrylate) at a water interface. J Phys Chem B. 2010;114:3457–60.

25. Butt H-J, Graf K, Kappl M. Physics and chemistry of interfaces. Weinheim: Wiley-VCH Verag, 2006.

26. Jasper JJ. The surface tension of pure liquid compounds. J Phys Chem Ref Data. 1972;1:841–1009.

27. Roe R-J. Surface tension of polymer liquids. J Phys Chem. 1968;72:2013–7.

28. Dee GT, Sauer BB. The surface tension of polymer liquids. Adv Phys. 1998;47:161–205.

29. Brandrup J, Immergut EH, Grulke EA Polymer Handbook 4th Edition. New York: John Wiley & Sons,1999.

30. DataPhysics Instruments GmbH, http://www.dataphysicsde/

31. Han S, Kim C, Kwon D. Thermal/oxidative degradation and stabilization of polyethylene glycol. Polym (Guildf). 1997;38:317–23.

32. Kchaou M, Alcouffe P, Chandran S, Cassagnau P, Reiter G, Al Akhrass S. Tuning relaxation dynamics and mechanical properties of polymer films of identical thickness. Phys Rev E. 2018;97:032507.

33. Chandran S, Handa R, Kchaou M, Al Akhrass S, Semenov AN, Reiter G. Time allowed for equilibration quantifies the preparation induced nonequilibrium behavior of polymer films. ACS Macro Lett. 2017;6:1296–1300.

34. Paeng K, Ediger MD. Molecular motion in free-standing thin films of poly(methyl methacrylate), poly(4-tert-butylstyrene), poly (alpha-methylstyrene), and poly(2-vinylpyridine). Macromolecules. 2011;44:7034.

35. Geng K, Chen F, Tsui OKC. Molecular-weight dependent Tg depression of silica-supported poly(α-methyl styrene) films. J Non-Cryst Solids. 2015;407:296–301.

36. Weyer S, Huth H, Schick C. Application of an extended Tool-Narayanaswamy-Moynihan model. Part 2. Frequency and cooling rate dependence of glass transition from temperature modulated DSC. Polym (Guildf). 2005;46:12240–6.

37. Schawe JEK. Vitrification in a wide cooling rate range: the relations between cooling rate, relaxation time, transition width, and fragility. J Chem Phys. 2014;141:184905.

38. Lee L-H. Correlation between Lewis acid-base surface interaction components and linear solvation energy relationship solvatochromic α and β parameters. Langmuir. 1996;12:1681–7.

39. Girifalco LA. A theory for estimation of surface and inerfacial energies. III. Estimation of surface energies of solids from contact angle data. J Phys Chem. 1960;64:561–5.

40. Lurio L, Kim H, Ruhm A, Basu J, Lal J, Sinha S, et al. Surface tension and surface roughness of supported polystyrene films. Macromolecules. 2003;36:5704–9.

41. McHale G, Newton M, Shirtcliffe N. Dynamic wetting and spreading and the role of topography. J Phys Condens Matter. 2009;21:464122.

42. Huang D, McKenna GB. New insights into the fragility dilemma in liquids. J Chem Phys. 2001;114:5621–30.

43. Evans CM, Deng H, Jager WF, Torkelson JM. Fragility is a key parameter in determining the magnitude of Tg-confinement effects in polymer films. Macromolecules. 2013;46:6091–103.

44. Sasaki T, Ichimura M, Irie S. Correlation between fragility and cooperativity in segmental dynamics of glass-forming para-substituted polystyrenes. Polym J. 2015;47:687–94.

45. Kramers HA. Brownian motion in a field of force and the diffusion model of chemical reactions. Physica. 1940;7:284–304.

46. Helfand E. Theory of the kinetics of conformational transitions in polymers. J Chem Phys. 1971;54:4651–61.